R.W. Hertzberg "Def. Frac. Mech. Eng. Mater." John Wiley Sons, 4ed, 1995

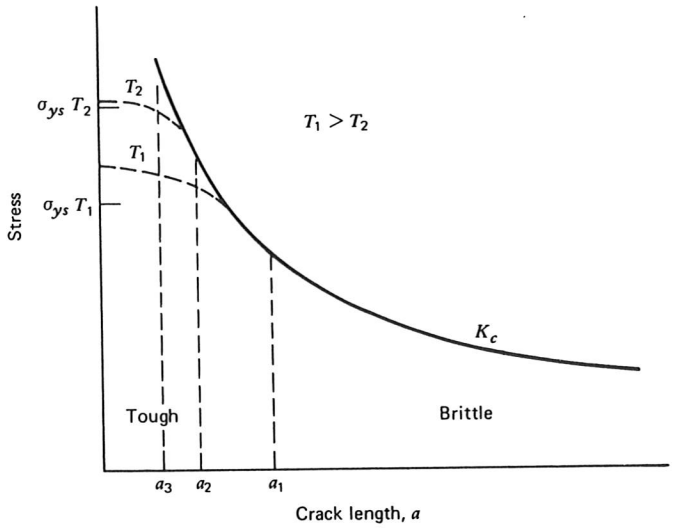

FIGURE 9.15 Schematic diagram showing relation between allowable stress level and flaw size. Solid line represents material fracture toughness K_c; dashed lines show effect of plasticity.

From the above discussion, it becomes apparent that a wide range of ''transition temperatures'' can be obtained simply by changing the specimen thickness and/or the crack length of the test bar. For this reason, transition temperature values obtained in the laboratory bear little relation to the performance of the full-scale component, thereby necessitating a range of correction factors as discussed earlier.

As mentioned above, the onset of brittle fracture is not always accompanied by the occurrence of the cleavage microscopic fracture mechanism. Rather, it should be possible to choose a specimen size for a given material, and tailor both thickness and planar dimensions such that a temperature-induced transition in energy to fracture, amount of lateral contraction, and macroscopic fracture appearance would occur *without the need for a microscopic mechanism transition.* Figure 9.16, from the work of Begley,[18] is offered as proof of this statement. Substandard thickness Charpy bars of 7075-T651 aluminum alloy were tested and shown to exhibit a temperature-induced transition in impact energy and fracture appearance. From Fig. 9.4, no such transition was observed when standard Charpy specimens of an aluminum alloy were broken.

9.4 IMPACT ENERGY—FRACTURE-TOUGHNESS CORRELATIONS

Although handicapped by the inability to bridge the size gap between small laboratory sample and large engineering component, the Charpy test sample method does possess certain advantages, such as ease of preparation, simplicity of test method, speed, low cost in test machinery, and low cost per test. Recognizing these factors, many researchers have attempted to modify the test procedure to extract more fracture information and seek possible correlations between Charpy data and fracture-toughness values obtained from fracture mechanics test samples. In one such approach, Orner

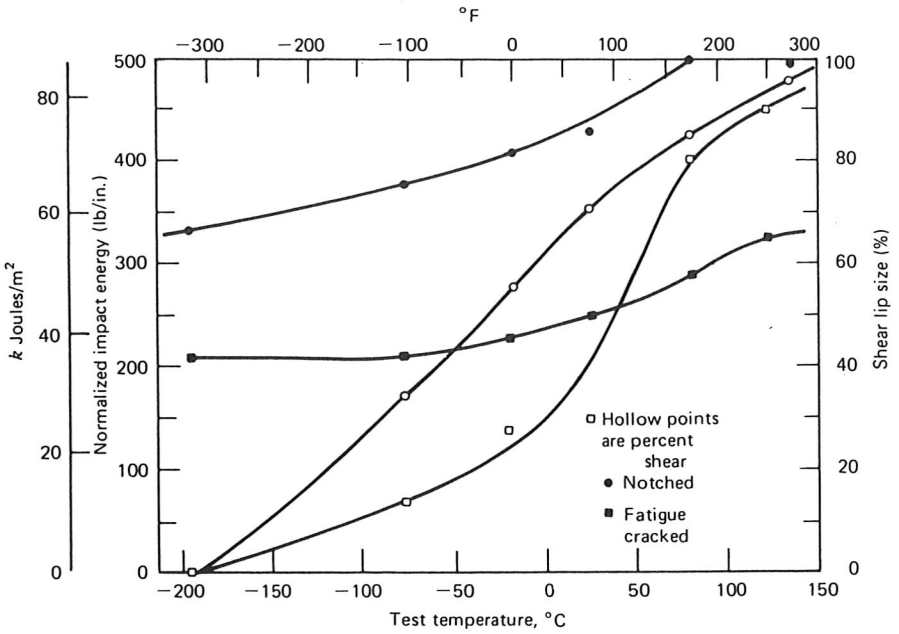

FIGURE 9.16 Charpy impact data for subsize specimen revealing transition temperature response in 7075-T651 aluminum alloy.[18] (Courtesy James A. Begley.)

and Hartbower[19] precracked the Charpy sample so that the impact energy for failure represented energy for crack propagation but not energy to initiate the crack.

$$E_T = E_i + E_p \tag{9-1}$$

where E_T = total fracture energy
E_i = fracture initiation energy
E_p = fracture propagation energy

They found that a correlation could be made between the fracture toughness of the material $\mathcal{G}_c$ and the quantity W/A, where W is the energy absorbed by the precracked Charpy test piece and A the cross-sectional area broken in the test. Although promising results have been observed for some materials (for example, see Fig. 9.17), the applicability of this test method should be restricted to those materials that exhibit little or no strain-rate sensitivity, since dynamic Charpy data are being compared with static fracture-toughness values. Also, the neglect of kinetic energy absorption by the broken samples as part of the energy-transfer process from the load pendulum to the specimen makes it impossible to develop good data in brittle materials where the kinetic energy component is no longer negligible.[20] Orner and Hartbower did point out, however, that the precracked Charpy sample could be used to measure the strain-rate sensitivity of a given material by conducting tests under both impact and slow bending conditions. Barsom and Rolfe[21] have verified this hypothesis with a direct comparison of static and dynamic test results from precracked Charpy V-notch (CVN) and plane-strain fracture-toughness samples, respectively. First, they established the strain-rate-induced shift in transition temperature for several steel alloys in the strength

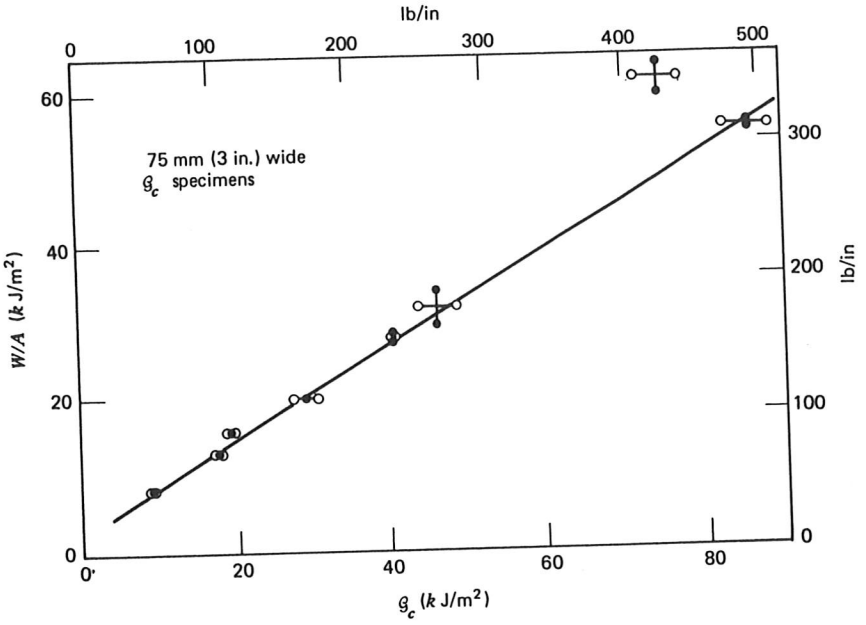

FIGURE 9.17 Relation between fatigue-cracked V-notch Charpy slow bend and $\mathcal{G}_c$ in a variety of 3.2-mm (0.125-in.)-thick aluminum alloys.[19] (Reprinted from *Welding Journal* by permission of the American Welding Society.)

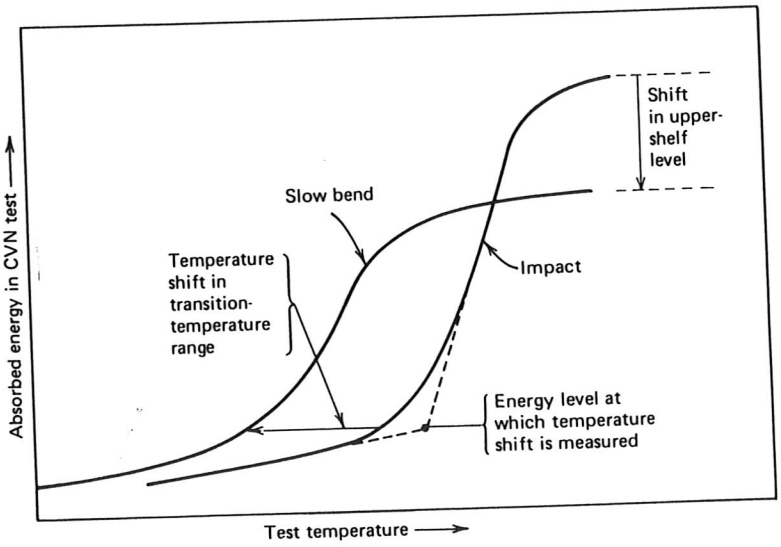

FIGURE 9.18 Diagram of impact energy versus test temperature revealing shift in transition temperature due to change in strain rate. (Note the higher shelf energy resulting from dynamic loading conditions, which may be related to a strain-rate-induced elevation in yield strength.)[21] (Reprinted by permission of the American Society for Testing and Materials from copyright material.)

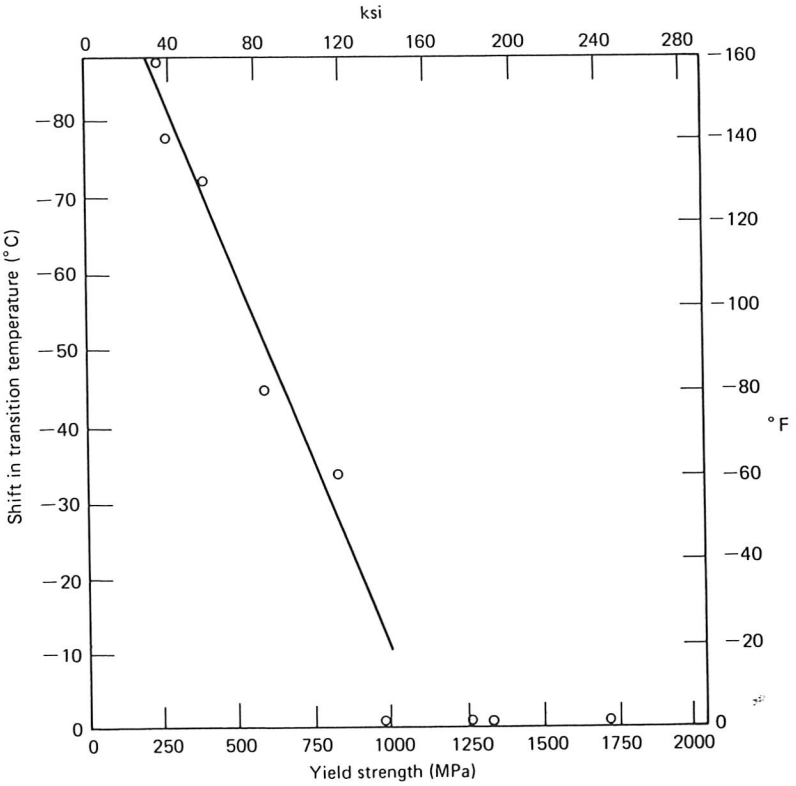

FIGURE 9.19 Effect of yield strength on shift in transition temperature between impact and slow bend CVN tests.[21] (Reprinted by permission of the American Society for Testing and Materials from copyright material.)

range of 275 to 1725 MPa (Figs. 9.18 and 9.19 and Table 9.2). They noted that the greatest transition temperature shift was found in the low-strength steels and no apparent strain-rate sensitivity was present in alloys with yield strengths in excess of 825 MPa. When these same materials were tested to determine their plane-strain fracture-toughness value, a corresponding shift was noted as a function of strain rate.

Figures 9.20*a* and 9.20*b* show static (K_{IC}) and dynamic (K_{ID}) plane-strain fracture-

TABLE 9.2 Transition Temperature Shift Related to Change in Loading Rate[21]

	σ_{ys}		Shift in Transition Temperature	
Steel	MPa	(ksi)	°C	(°F)
A36	255	(37)	−89	(−160)
ABS-C	269	(39)	−78	(−140)
A302B	386	(56)	−72	(−130)
HY-80	579	(84)	−44	(−80)
A517-F	814	(118)	−33	(−60)
HY-130	945	(137)	0	(0)
10Ni–Cr–Mo–V	1317	(191)	0	(0)
18Ni (180)	1241	(180)	0	(0)
18Ni (250)	1696	(246)	0	(0)

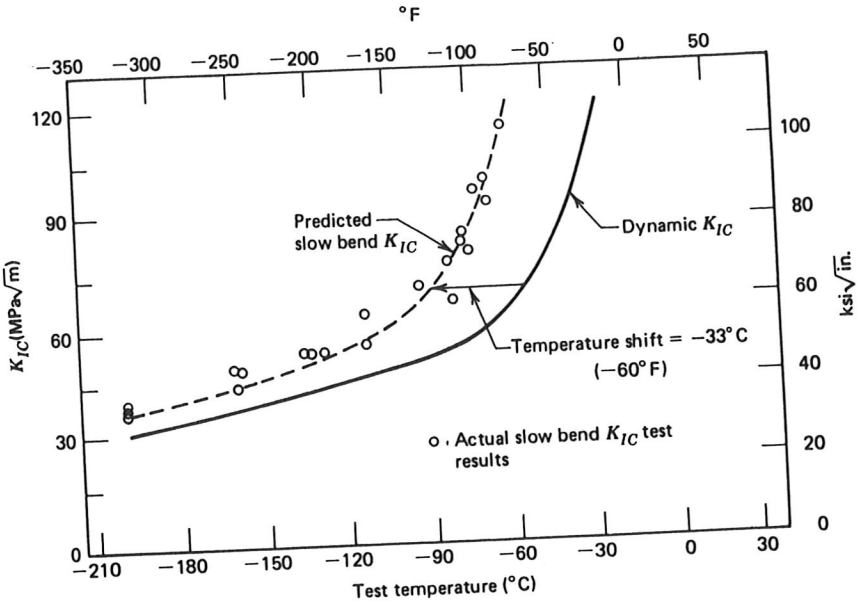

(*a*)

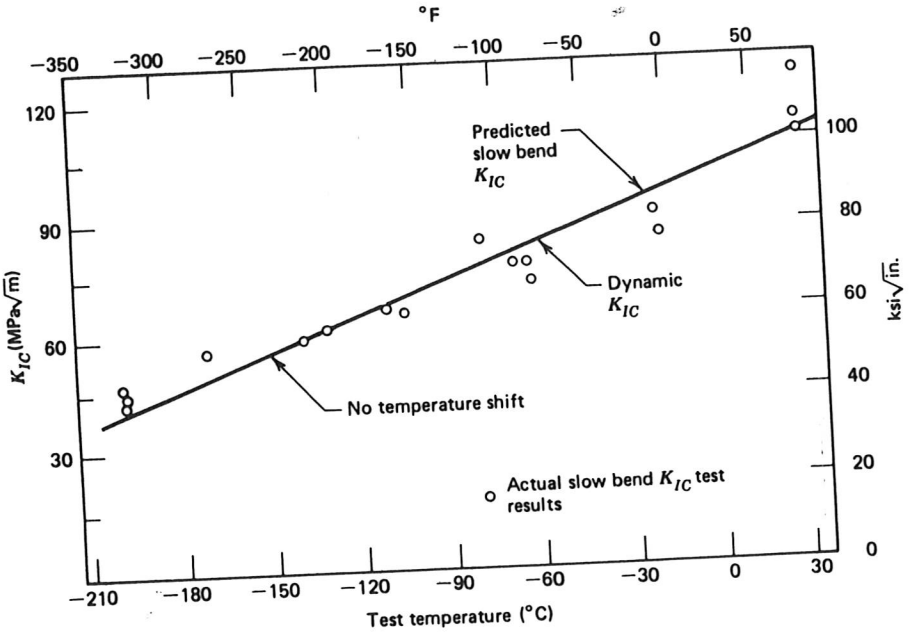

(*b*)

FIGURE 9.20 Use of CVN test results to predict the effect of loading rate on K_{IC}. (*a*) A517-F steel.[21] (*b*) 18Ni-(250) maraging steel. (Reprinted by permission of the American Society for Testing and Materials from copyright material.)

toughness values plotted as a function of test temperature. One additional point should be made with regard to these data. Although K_{IC} increased gradually with temperatures for the high-strength steels, a dramatic transition to higher values was observed for the low- and intermediate-strength alloys. It should be emphasized that this transition was not associated with the plane-strain to plane-stress transition, since all the data reported represented valid plane-strain conditions. A similar transition in plane-strain ductility (measured with a thin, wide sample) occurred in the same temperature region, but no such transition developed in axisymmetric ductility (measured with a conventional round tensile bar). This tentative correlation between the K_{IC} and plane-strain ductility transitions was strengthened with the observation that both transitions were associated with a fracture mechanism transition from cleavage at low temperatures to microvoid coalescence at high test temperatures.[22,23]

It is seen that the toughness levels of both strain-rate sensitive and insensitive materials increased with increasing temperature (Figs. 9.20*a* and 9.20*b*). Of significance is the fact that the predicted static K_{IC} values (broken line), obtained by applying the appropriate temperature shift (Fig. 9.19) to the dynamic test results (solid line), were confirmed by experimentation. Since dynamic plane-strain fracture-toughness testing procedures are more complex and beyond the capability of many laboratories, estimation of K_{ID} from more easily determined K_{IC} values represents a potentially greater application of the strain-rate-induced temperature shift in the determination of fracture properties.

Additional efforts have focused on developing empirical relations between impact energy absorbed in DT[17] and Charpy[21] specimens and K_{IC} values. Two such relations are shown in Figures 9.21 and 9.22 with additional correlations given in Table 9.3. It is to be noted that these relations vary as a function of material, the test temperature range, notch acuity, and strain rate. For example, these correlations are different in the upper-shelf energy regime as compared with the transition zone; they depend also on whether the Charpy specimen is precracked and whether it is impacted or tested at slow strain rates. Roberts and Newton[24] examined the accuracy of 15 such relations and concluded that no single correlation could be used with any degree of confidence to encompass all possible test conditions and differences in materials. Furthermore, because of the intrinsic scatter associated with K_{IC} and CVN measurements, the correlations possessed a relatively wide scatter band. Roberts and Newton also pointed out that some of the K_{IC} values used to establish these correlations were invalid with respect to E399-81 test requirements, and that CVN values tended to vary according to the CVN specimen location in the plate.

In addition to these difficulties, certain additional basic problems must not be overlooked. For example, the K_{IC}–CVN correlation implies that you can directly compare data from blunt and sharp notched samples and data from statically and dynamically loaded samples, respectively. The latter difficulty may not be too important for the materials shown in Fig. 9.22 since they all have yield strengths greater than 825 MPa (except A517-F) where strain-rate effects are minimized (see Fig. 9.19 and Table 9.2). The same probably holds true for the DT–K_{IC} data in Fig. 9.21, since only high-strength materials are shown. When the material's fracture properties are sensitive to strain rate, however, a two-step correlation between impact CVN data and K_{IC} values is recommended. First, K_{ID} values are inferred from impact CVN data with the aid of an appropriate correlation (e.g., see Table 9.3). Then K_{IC} is estimated from

ksi$\sqrt{\text{in.}}$

K_{IC}. (*a*)
American

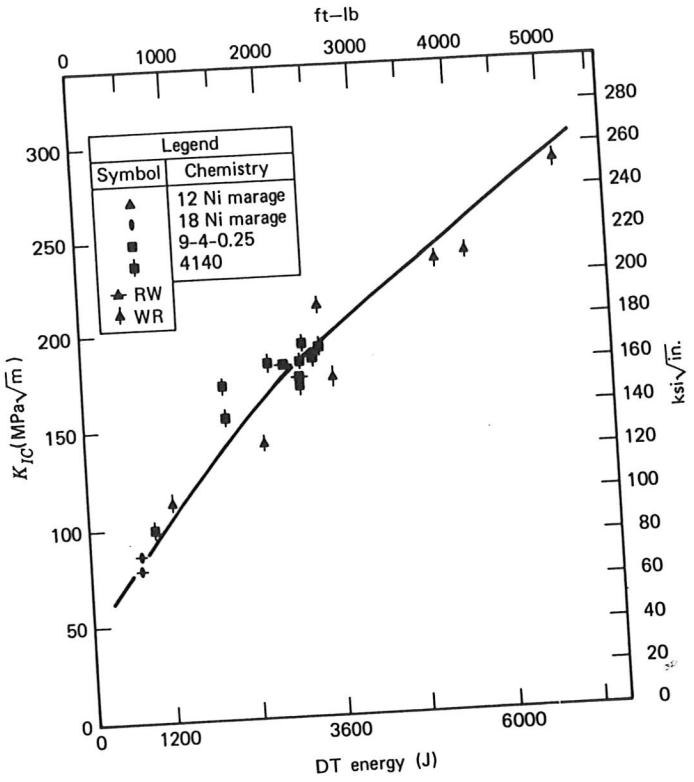

FIGURE 9.21 Relation between 2.5-cm dynamic tear energy and K_{IC} values of various high-strength steels.[17] (Reprinted by permission of the American Society for Testing and Materials from copyright material.)

K_{ID} data through the use of the temperature shift factor (Fig. 9.19). Finally, fracture mechanics—impact energy correlations for engineering plastics have been reported and are reviewed elsewhere.[11]

9.5 INSTRUMENTED CHARPY IMPACT TEST

In recent years, considerable attention has been given to instrumenting the impact hammer in the Charpy machine pendulum so as to provide more information about the load-time history of the sample during the test.[28,29] A typical load-time trace from such a test is shown in Fig. 9.23. A curve of this type can provide information concerning the general yield load, maximum and fracture loads, and time to the onset of brittle fracture. To determine the fracture energy of the sample requires integration of a load-*displacement* record. However, it is possible to calculate the fracture energy from a load-*time* curve if the pendulum velocity is known. Assuming this velocity to be constant throughout the test, the fracture energy is computed to be

$$E_1 = V_0 \int_0^t P dt \tag{9-2}$$